Application of Ground Penetrating Radar in Road Engineering Inspection

Huilin Liu[1,2], Yilong Zhang[1,2], Haowen Wen[1,2], Jianyu Wu[1,2,*], and Weiliang Zhang[1,2]

[1]Guangdong Traffic Engineering Quality Testing Center of Building Academy Co., Ltd., Guangzhou, 510550, China
2Guangdong Province Traffic Infrastructure Intelligent Detection Engineering Technology Research Center, Guangzhou, 510550, China
*Corresponding author: Jianyu Wu; E-mail: 21121121@bjtu.edu.cn

Abstract. With the continuous expansion of highway construction, quality control during construction and the reliability of subsequent operation and maintenance have drawn increasing attention. Ground Penetrating Radar (GPR), as an efficient, precise, and non-destructive testing technique, has been widely applied in road engineering. This paper systematically expounds the electromagnetic wave propagation theory, antenna frequency selection, and dielectric modeling methods of GPR, and analyzes its applications in pavement layer thickness measurement, subsurface defect identification, underground pipeline detection, and tunnel lining quality inspection. Taking the emergency inspection of an embankment collapse on a radial road in Guangzhou as an engineering case study, the paper details the practical effectiveness of GPR in rapidly detecting subsurface voids after road collapse, conducting continuous multi-day dynamic monitoring, and performing borehole verification. The inspection results show that 17 anomalous zones were identified during the emergency inspection period, with the largest composite anomalous area reaching approximately 472 m², and the borehole verification accuracy reaching 90%, confirming the technical advantages of GPR in emergency subsurface defect inspection. Meanwhile, the case study reveals applicability boundaries such as severe radar signal attenuation in high-moisture environments and strong reflection interference from heterogeneous gravel fill layers. The study demonstrates that GPR can effectively improve the refinement level of road construction and maintenance quality control, though the detection depth is limited under high-moisture conditions. It is recommended to integrate multi-source data fusion methods to enhance detection reliability under complex working conditions.

Keywords: Non-Destructive Testing, Ground Penetrating Radar, Highway Construction, Quality Control, Subsurface Defects, Emergency Inspection.

1 Introduction

As a core component of modern comprehensive transportation networks, the construction quality of ordinary highways directly affects operational safety and long-term service performance. Traditional methods for internal pavement quality inspection, such

© The Author(s) 2026
H. Wu et al. (eds.), *Proceedings of the 2026 3rd International Conference on Civil Engineering Structures and Concrete Materials (CESCM 2026)*, Advances in Engineering Research 312,
https://doi.org/10.2991/978-94-6239-865-8_7

as core drilling, suffer from inherent shortcomings including low inspection efficiency, insufficient sample representativeness, and structural damage to existing pavement. These methods are increasingly inadequate for meeting the high-precision and rapid inspection demands of large-scale engineering projects. Ground Penetrating Radar (GPR) emits high-frequency electromagnetic waves in a non-contact manner and receives reflection signals from interfaces of different subsurface media, enabling large-area continuous scanning of pavement structures without interrupting normal traffic. GPR has thus become a core technique in modern road engineering non-destructive testing[1–3].

In recent years, scholars worldwide have conducted extensive systematic research on automatic GPR data interpretation, three-dimensional imaging, and multi-frequency cooperative detection[4–6]. However, systematic studies summarizing typical engineering application scenarios—particularly rapid emergency inspection after road collapse disasters—remain relatively scarce. Based on the fundamental technical principles of GPR and incorporating the actual engineering case of an emergency inspection of an embankment collapse on a radial road in Guangzhou, this paper systematically discusses the core application scenarios, technical advantages, and applicability boundaries of GPR in road construction quality control and operational maintenance inspection.

2 Theoretical Foundations of GPR Detection Technology

Ground Penetrating Radar is a non-destructive testing technique based on the principle of electromagnetic wave reflection. Its core theory encompasses three aspects: electromagnetic wave propagation behavior, antenna design, and dielectric modeling.

2.1 Electromagnetic Wave Propagation Characteristics

GPR transmits high-frequency electromagnetic waves (commonly in the 10 MHz–3 GHz band) into the ground via a transmitting antenna. When these waves encounter interfaces between media with different dielectric constants, reflection, refraction, and scattering occur. The receiving antenna records the reflected echo signals, which are then used to invert subsurface structural information.Among the dielectric properties, the relative permittivity (ε_r) is the key parameter governing electromagnetic wave propagation: the greater the permittivity contrast across an interface, the higher the reflection coefficient and the stronger the reflected signal. The reflection coefficient R is given by:

$$R=\frac{\sqrt{\varepsilon_1}-\sqrt{\varepsilon_2}}{\sqrt{\varepsilon_1}+\sqrt{\varepsilon_2}} \tag{1}$$

where ε_1 and ε_2 are the relative permittivities of the adjacent media.

For asphalt concrete pavements, the material is characterized as a two-phase discrete random medium composed of aggregates, asphalt mastic, air voids, and backfill materials. When electromagnetic waves propagate through such media, scattering effects

arise from the spatially heterogeneous permittivity distribution, causing the signal waveforms to exhibit random characteristics. Furthermore, for shallow-depth detection (< 3 m), the antenna radiation pattern, dielectric loading effects, and ambient electromagnetic environment must be considered. The geometry of bow-tie antennas, shielding enclosure design, and subsurface dielectric properties all significantly alter the electromagnetic wave field distribution.

2.2 Antenna Frequency and Detection Performance

The selection of antenna center frequency directly determines the trade-off between detection depth and resolution. High-frequency antennas (e.g., 1 GHz, 2 GHz) have short wavelengths and high resolution, making them suitable for fine inspection of pavement structural layers. Low-frequency antennas (e.g., 100 MHz, 200 MHz, 400 MHz) offer greater penetration depth, making them suitable for detecting deep-seated subgrade defects. Taking the GSSI SIR series GPR as an example, extensive inspection practice has shown that high-frequency antennas can achieve vertical resolution of ±3 mm for shallow road targets, while low-frequency antennas provide a higher signal-to-noise ratio for deep detection beyond 3 m. In practice, multi-frequency antenna combinations are commonly adopted to balance shallow resolution and deep penetration. A typical field setup for measuring total pavement thickness using the short pulse radar method is shown in Fig. 1.

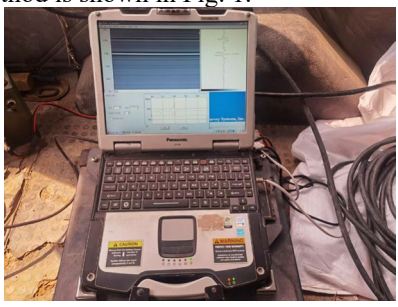




Fig. 1. Measuring total pavement thickness using short pulse radar method.

The pavement thickness inspection case from the surface reconstruction project on Provincial Highway S121, spanning from the Xicun Industrial Zone in Shunde District to the south side of Longjiang No. 2 Bridge, provides direct engineering evidence for high-frequency antenna selection criteria.he project is located in Lecong Town, Shunde District, Foshan City, covering the chainage range K45+750 to K49+450. It is a Class I highway with dual urban road functionality, configured as a dual three-lane carriageway. Following treatment of the existing pavement, the left carriageway was overlaid with 4 cm of improved-gradation GAC-13C modified asphalt concrete, while the right carriageway received 4 cm of GAC-13C modified asphalt concrete plus 5 cm of AC-20C conventional asphalt concrete.The inspection employed a GSSI SIR-series GPR system (USA) equipped with a 2.0 GHz center-frequency high-frequency shielded antenna. Prior to inspection, core drilling calibration determined the electromagnetic

wave propagation velocity in the asphalt concrete to be 11.76 cm/ns. A 310 m test section (K45+750 to K46+060) was surveyed, with thickness values averaged at 10 m intervals, yielding a total of 186 measurements. The detection results are summarized in Table 1. For the left carriageway, 93 measurement points with a design thickness of 40 mm showed measured thicknesses ranging from 39 mm to 80 mm, with a mean of 54.4 mm. All points satisfied the compliance threshold of ≥36.0 mm, resulting in a 100% compliance rate. For the right carriageway, 93 measurement points with a design thickness of 50 mm showed measured thicknesses ranging from 43 mm to 128 mm, with only one point failing to meet the compliance threshold of ≥45.0 mm, yielding a 98.9% compliance rate.This case study demonstrates that the 2.0 GHz high-frequency antenna can clearly resolve two surface layer structures of different design thicknesses, achieving millimeter-level vertical resolution. All measurement points could be surveyed and processed within a single day, covering a total lane length of 1.86 km without requiring traffic interruption.

Table 1. Summary table of total thickness detection results of asphalt pavement by road sections.

Sub-project	Qualified Value (mm)	Mean (mm)	Std. Dev. (mm)	Representative Value (mm)	No. of Test Points	No. of Qualified Points	Pass Rate (%)
Left Section K45+750~K46+060 Asphalt Concrete Pavement	36	54.4	7.96	53	93	93	100
Right Section K45+750~K46+060 Asphalt Concrete Pavement	45	76.2	20.31	72.7	93	92	98.9

2.3 Numerical Simulation and Dielectric Modeling

To optimize detection performance and establish defect identification criteria, it is necessary to construct dielectric models that reflect actual material characteristics for forward simulation. The Finite-Difference Time-Domain (FDTD) method can effectively simulate GPR wave field propagation in random media and analyze the electromagnetic response characteristics of typical defects such as cracks, voids, and water-rich zones [7-8]. The two-phase discrete random medium model can accurately characterize the permittivity distribution of asphalt concrete, providing a theoretical basis for GPR data inversion and interpretation.

3 Applications of GPR in Road Inspection

3.1 Pavement Layer Thickness Measurement

Asphalt concrete pavements are designed and constructed in a layered structure. GPR can achieve large-area rapid inspection without disrupting traffic and has been widely applied in pavement layer thickness assessment. In the radar images of normal road sections, the reflection events or chromatographic bands of each structural layer appear as nearly horizontal linear features, with essentially consistent signal intensity within layers. However, even for asphalt surface courses paved in lifts, variations in material composition and construction quality among individual lifts still exist, producing dielectric discontinuities at layer interfaces that appear as a continuous reflection event or chromatographic line. A typical example is shown in Fig.2.

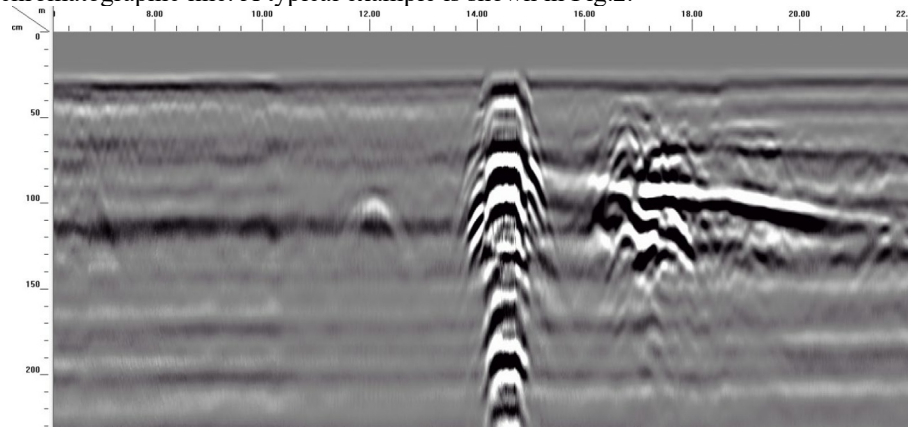


Fig. 2. GPR image of pavement structural layers on a normal road section (SIR-20 system with 2 GHz antenna).

GPR determines layer thickness using the two-way travel time method, given by:

$$h = \frac{c\Delta t}{2\sqrt{\varepsilon}} \tag{2}$$

where c is the speed of light in vacuum (approximately 3×10^8 m/s), Δt is the two-way travel time of the electromagnetic wave within the layer, and ε is the relative permittivity of the layer material.

Conventional methods typically calibrate the permittivity at a single point through core drilling and then extrapolate it as a fixed value across the entire pavement section. However, in practice, factors such as material segregation and uneven compaction produce significant spatial heterogeneity in pavement permittivity. Existing research has shown that by fitting the permittivity values of calibration-section measurement points using a normal distribution (mean μ, standard deviation σ) and subsequently constructing a thickness acceptance probability model, the thickness measurement accuracy of GPR can be improved to the millimeter level.

In an overlay rehabilitation project on a Class I highway, the SIR-4000 system with a 2 GHz antenna was used to inspect a 2 km test section for thickness. Five locations were identified where the surface course thickness failed to meet the design requirement (design thickness 12 cm; measured thickness 9–10 cm). After confidence-level correction, the measurement error of this method was reduced to ±1.5 mm, and the section acceptance qualification rate improved to 98%.

3.2 Subsurface Defect Detection

When the bonding condition between the pavement surface and the base course is sound, the permittivity contrast between the two is small, resulting in a weak interlayer reflection signal with smooth and regular waveforms. If surface water infiltrates through cracks, dynamic water pressure generated under repeated vehicle loading causes gradual loosening of the interlayer bond between the surface and base courses. In localized areas, void defects may even develop. Typical GPR images of such defects are shown in Fig.2 and Fig.3. Different types of subsurface defects exhibit distinct waveform and reflection-event response characteristics in GPR images:

Water-rich zones: The reflection signal at the top of the defect body is distinct. Due to the rapid attenuation of electromagnetic waves in water, the reflection signal intensity below the top interface is weak. The phase of the top-interface reflected wave in the water-rich anomalous zone is consistent with the incident wave, whereas the phase of the bottom-interface reflected wave is opposite to the incident wave. The continuity of reflection events is poor. These conditions lead to increased subgrade moisture content, reduced structural strength, decreased bearing capacity, and the potential for further void or cavity formation in surrounding areas.

Loosened soil zones: The lateral continuity of reflection events is interrupted, the waveform structure is disordered and irregular, and the reflection amplitude is moderate. The defect characteristics include high soil porosity, insufficient compaction, poor structural uniformity, low overall strength, and high compressibility.

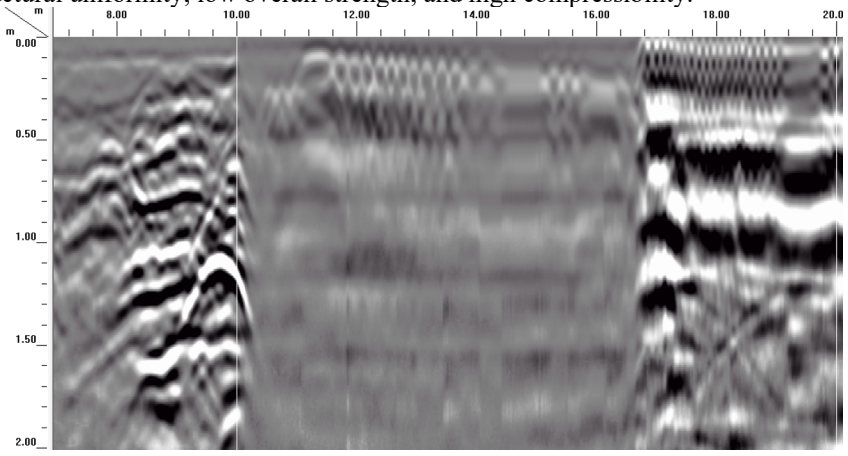


Fig. 3. GPR image of loosened soil defect in road subgrade (SIR-4000 system with 400 MHz antenna).

Voids: The shallow stratum exhibits weak reflection characteristics with disrupted reflection events. Two clearly distinguishable reflection interfaces are present, with irregular strong reflections developing between layers. The waveforms are disordered and the reflection amplitude is significantly increased. The defect characteristic is separation between the structural layer and the soil base, with a post-separation clearance of less than 50 cm and generally shallow burial depth. A typical GPR image of a subsurface void defect is shown in Fig. 4.

Cavities: The overall cavity zone is characterized as a weak reflector, accompanied by multiple combined reflection response features. The defect characteristic is a clearance of at least 50 cm after separation between the structural layer and soil base, or an internally developed cavity within the soil mass. Typically, the upper portion is a void zone and the lower portion a loosened soil zone, posing a serious threat to engineering structural stability.

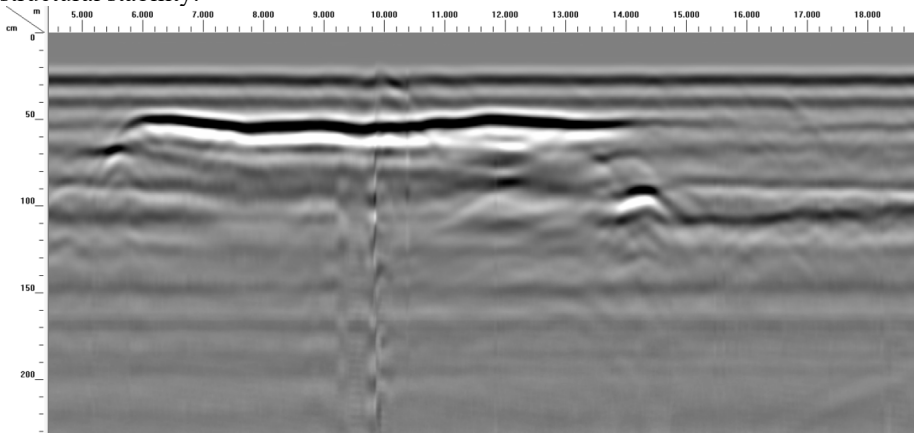


Fig. 4. GPR image of subsurface void defect (SIR-4000 system with 400 MHz antenna).

3.3 Underground Pipeline and Infrastructure Detection

With the accelerating pace of urbanization, the number of underground pipelines has increased dramatically. However, due to issues such as missing pipeline records and aging infrastructure, construction-related damage incidents occur frequently. GPR identifies target objects by exploiting the permittivity contrast between pipeline materials and the surrounding soil, offering advantages of high efficiency, non-destructiveness, and high resolution. It has become one of the mainstream techniques for underground pipeline inspection. By extension, this technology can also be applied to the detection of underground building structures and civil air defense works. Typical radar images are shown in Fig.5-Fig.7.

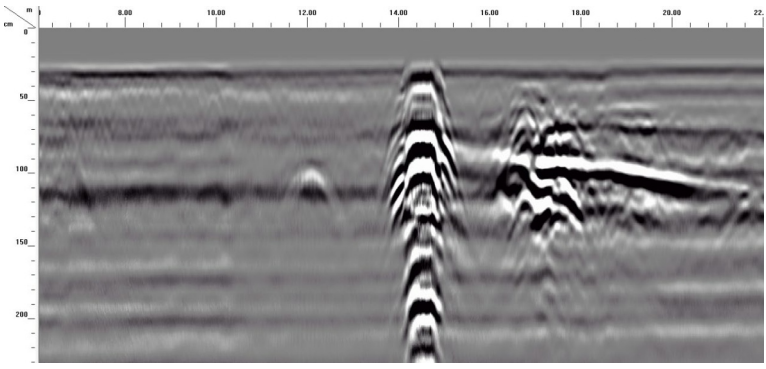


Fig. 5. GPR image of underground pipeline: sewage well (SIR-4000 system with 400 MHz antenna).

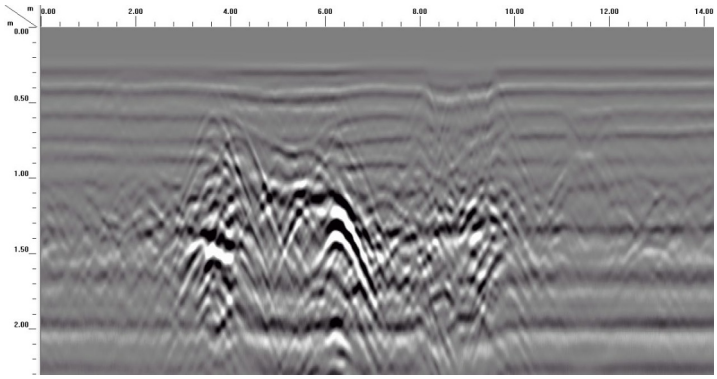


Fig. 6. GPR image of underground pipeline: metal pipelines (SIR-4000 system with 400 MHz antenna).

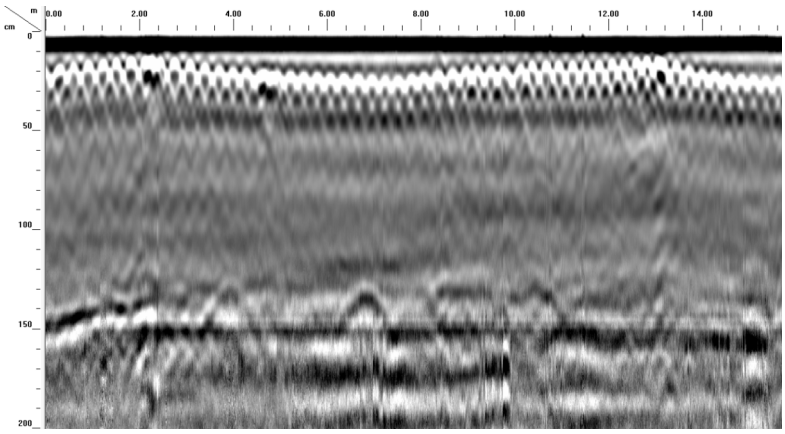


Fig. 7. GPR image of underground pipeline: Reinforcement and upper interface of retaining wall toe (SIR-4000 system with 400 MHz antenna).

3.4 Tunnel Engineering Inspection

During tunnel excavation, adverse geological bodies ahead of the tunnel face (such as faults, fracture zones, and karst cavities) frequently cause collapse and water inrush accidents, resulting in casualties and equipment damage. Therefore, timely identification of the scale and distribution of adverse geological structures ahead of the tunnel face is of great significance for formulating appropriate excavation schemes and support measures. GPR is commonly used for advance geological prediction in tunnels, often combined with seismic reflection methods (e.g., TSP) for comprehensive assessment. The effective prediction range of the GPR method is generally 20 m.

As the primary load-bearing and waterproofing structure of a tunnel, the construction quality of the lining is critical to the long-term stability of the tunnel. GPR can detect key indicators including lining thickness (primary support and secondary lining), lining compactness, voids behind the lining, and the position and quantity of arch frames and reinforcement. A typical GPR image is shown in Fig.8.

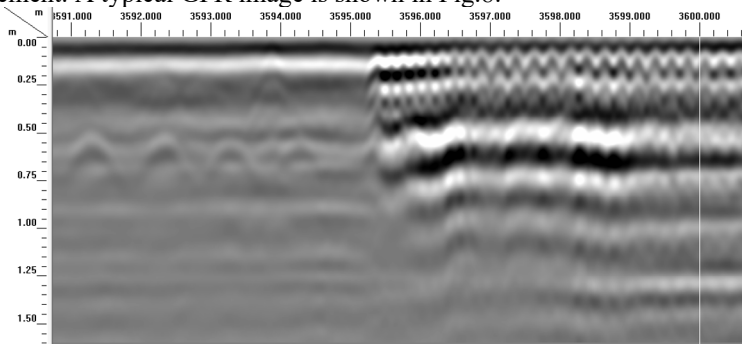


Fig. 8. GPR image of tunnel lining (SIR-4000 system with 400 MHz antenna).

4 Engineering Case Study: Emergency GPR Inspection of an Embankment Collapse on a Radial Road in Guangzhou

4.1 Engineering Background and Inspection Plan

A collapse occurred on the auxiliary road surface of an extended embankment section between bridge abutments of a radial road in Guangzhou. The collapse area measured 17 m × 6.5 m, with a depth of approximately 4 m. An emergency special inspection and monitoring program was initiated for the main carriageway of this road section. The emergency inspection employed the GSSI SIR-4000 GPR system (USA) configured with a 400 MHz center-frequency shielded antenna. Survey line layout and data acquisition were conducted in accordance with the Technical Specification for Radar Detection of Road Collapse Hazards (T/CMEA 2-2018). The inspection coverage encompassed the collapse-affected zone (approximately 60 m longitudinally, spanning 4 lanes), and multiple rounds of repeated inspection were carried out to track the development of subsurface defects.

4.2 GPR Inspection Results

The emergency inspection was conducted from 12:00 on August 6 to 11:00 on August 12, 2024, lasting 7 days. The SIR-4000 GPR system with a 400 MHz shielded antenna was used to perform multiple rounds of repeated inspection over the designated collapse-affected zone. A total of 17 survey lines were laid out and dynamically adjusted according to site conditions and construction progress, with 16 inspection operations completed in total.

During the first inspection at 12:00 on August 6, five anomalous zones were identified in three lanes around the collapse area. The voids were mainly located at depths of 0.3–0.5 m and 0.6–0.9 m below the pavement surface, with a maximum vertical void extent of 0.35 m. Anomaly No.5 was the largest in scale, and voids were also detected in the crash barrier and corrugated guardrail areas. A follow-up inspection at 18:00 on the same day revealed that the number of anomalous zones had increased to 10, with newly detected anomalies concentrated around the crash barrier and the depth extending to 0.7–1.1 m. New void layers appeared in some areas, indicating that the subsurface defects were continuing to expand.

At 13:00 on August 7, a systematic scan covering 30 m ahead of and behind the collapse-affected zone was conducted. Five anomalies were identified within the three lanes, among which Anomaly No.5 was the largest and Anomaly No.1 the smallest, validating the high-resolution detection capability of GPR.

At 12:00 on August 8, the inspection showed that existing anomalies had connected and expanded. Anomaly No.5 and the newly identified Anomaly No.6 merged into a combined area of approximately 472 m², forming the largest composite anomalous zone of the inspection. By 23:00 on the same day, the number of anomalous zones had increased to 13, with newly detected anomalies mostly distributed in the second and third lanes on the right side, while the void depths remained concentrated within the previously identified range.

On August 9, as grouting operations progressed, the inspection coverage was extended to the opposite-side diversion strip area. At 11:30, four new anomalous zones were identified, one of which exhibited a maximum void extent of 0.25 m. A water-rich zone was detected at a depth of 0.8 m below the pavement surface near the construction area in the diversion strip. The 16:00 follow-up inspection produced results essentially consistent with the previous round, with no significant changes in the anomalies.

At 8:00 on August 10, the inspection revealed a longitudinal expansion trend in one water-rich zone, and accelerated grouting treatment was recommended. At 14:00 on August 11, affected by rainfall, the four newly identified anomalies in the diversion strip could not be inspected. In the remaining inspected areas, water-rich conditions were generally present at depths of 0.5–0.8 m below the pavement, and the electromagnetic wave signals were attenuated due to increased moisture content.

At 4:00 on August 12, the inspection showed that rainwater infiltration into the subgrade had created water-rich zones at depths of 0.4–0.6 m below the pavement surface, significantly interfering with radar signals. Apart from the grouted areas, no obvious voids were detected within 0.6 m of the pavement surface in the remaining originally

anomalous zones. At the final inspection at 11:00, under the combined influence of grouting and rainfall, the subsurface soil moisture content had increased substantially. Electromagnetic wave interference was severe below 0.6–0.9 m depth, resulting in poor detection performance. No obvious shallow voids were found in the original anomalies, and the results for the diversion strip zone remained essentially consistent with earlier findings.

In summary, a total of 17 anomalous zones were identified during the emergency inspection. The voids were mainly distributed across two depth intervals below the pavement surface. The number of anomalies progressively increased from 5 to 17 over the course of the inspection, with a maximum composite anomalous area of approximately 472 m² forming, reflecting the continuous expansion of subsurface voids under the combined action of traffic loading and hydrodynamic pressure. After grouting, the shallow voids were effectively filled. However, the increased moisture content caused by rainfall significantly degraded detection performance, confirming the technical limitation that GPR detection capability deteriorates under high-moisture conditions.

4.3 Verification Results of Rayleigh Wave Method

In road collapse emergency detection, to verify the accuracy of ground penetrating radar (GPR) results, the multichannel analysis of surface waves (MASW) method was introduced in parallel for cross-validation.The GPR survey employed a SIR-4000 main unit paired with a 400 MHz shielded antenna, completing 16 survey rounds within 7 days and cumulatively identifying 17 anomalous zones. The largest anomaly covered approximately 472 m². The identified voids were predominantly distributed in two depth intervals—0.3–0.5 m and 0.6–0.9 m beneath the pavement surface—highlighting the advantage of GPR in shallow high-resolution detection. However, owing to electromagnetic wave attenuation in high-moisture environments and strong reflection interference from non-uniform crushed stone layers, the GPR detection performance degraded below 0.6–0.9 m depth, limiting its ability to resolve medium-to-deep geological structures and deep karst conduits. This limitation motivated the introduction of the MASW method.The MASW survey employed a DZQ-24A engineering seismograph with 18 survey lines totaling 1,012 m in length, covering 217 measurement points. The investigation depth ranged from 2 to 20 m, addressing the detection gap left by GPR in the medium-to-deep range. This method yields a two-dimensional shear-wave (S-wave) velocity profile through inversion of surface-wave dispersion characteristics, and identifies unfavorable geological bodies via velocity contrast. In this survey, 17 low-velocity anomalies were detected and 5 hazard zones were delineated. Two major anomalies were inferred to correspond to a severely loose void zone and a moderately loose zone, respectively, both connected to deep karst fissures.

The results obtained from the two methods showed high spatial correspondence. The shallow voids identified by GPR and the deep karst fissures revealed by MASW were spatially coincident, indicating that the shallow voids represent the surface manifestation of upward-propagating deep karst conduits. Together, they constitute a cascading defect evolution pattern. Furthermore, MASW also revealed deep-seated hazards that GPR failed to detect. In this survey, although the shallow grouting effect in the collapse

zone was satisfactory, a funnel-shaped low-velocity anomaly persisted at depth, which likely remained connected to deep karst fissure conduits and had not yet been completely sealed. This finding provided critical evidence for guiding subsequent remediation. MASW accomplished the cross-validation of GPR results at three levels. First, the anomalous zones identified by the two methods exhibited high spatial consistency: the shallow voids detected by GPR and the deep karst fissures detected by MASW formed a vertically aligned hazard chain. Second, borehole findings simultaneously verified the interpretative accuracy of both geophysical methods—GPR achieved 90% accuracy, and the karst cavity locations inferred by MASW were fully consistent with borehole exposures. Third, MASW detected quantitative changes in S-wave velocity before and after grouting, which, from the perspective of improved soil mechanical properties, indirectly validated both the existence of the shallow void zones identified by GPR and the effectiveness of the remediation. The plan of comprehensive geophysical exploration results obtained by the Rayleigh wave method is shown in Fig. 9.

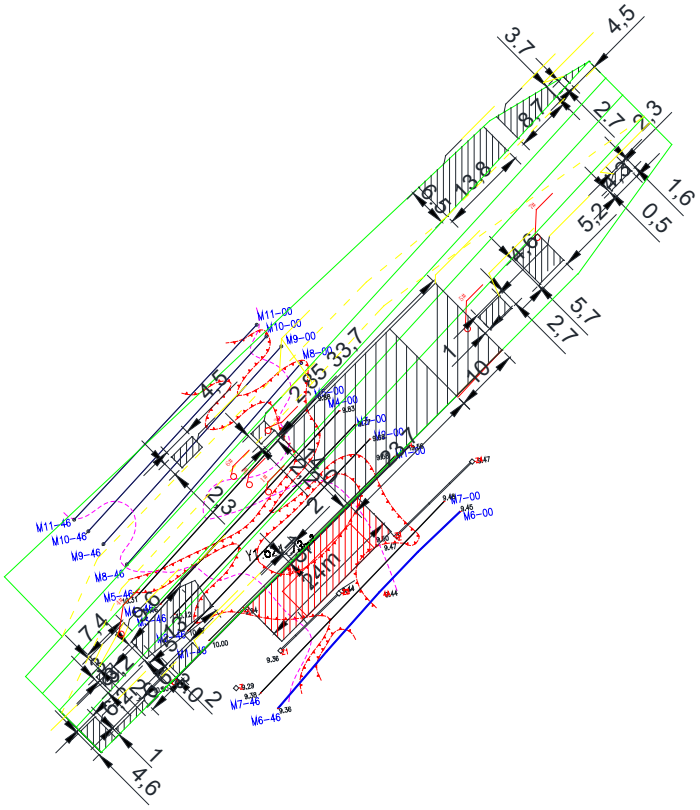


Fig. 9. Plan of Comprehensive Geophysical Exploration Results Using Rayleigh Wave Method

The above cross-validation confirms that GPR provides reliable detection accuracy and engineering practicality for road collapse emergency surveys. As a complementary tool for medium-to-deep investigation, MASW not only validates the correctness of

GPR shallow-detection results but also extends the investigation depth to reveal deep geological structures. The synergistic application of these two methods effectively enhances the coverage and reliability of subsurface defect detection under complex geological conditions.

4.4 Borehole Verification Results

To verify the accuracy of the GPR inspection results and ascertain the distribution of subsurface defects in and around the collapse zone, shallow borehole verification was conducted during this emergency inspection. A total of 16 boreholes were laid out, comprising 10 boreholes in the vicinity of the collapse zone and 6 outside this area.

Of the 10 boreholes near the collapse zone, 9 revealed loose strata or voids, corresponding to a GPR detection accuracy of 90%. For example, the inspection results for Borehole No.1 were consistent with the GPR findings, as shown in Fig. 10. The verification result for Borehole No.3, which revealed loose strata, is shown in Fig. 11.



Fig. 10. Borehole verification: Hole 1# (void).



Fig. 11. Borehole verification: Hole 3# (loose)

The stratigraphic profiles of individual boreholes showed that the pavement structure in the vicinity of the collapse zone generally consisted of a freshly poured concrete layer, a dense sand layer, and a lower loose layer. Multiple boreholes revealed different types of subsurface defects, and the results indicated that various subsurface defects—including voids, loosened zones, and water-rich zones—still existed in the area.

Of the 6 boreholes outside the collapse vicinity, 5 showed relatively dense strata, with only 1 exhibiting loosening and voids. In addition, a total of 8 boreholes encountered hard objects at a depth of 0.6–0.8 m, suggesting the possible presence of multiple zones of uncompacted gravel fill below this depth. This fill layer not only obstructed drilling but also interfered with GPR electromagnetic waves. Therefore, the possible existence of defects below this layer could not be ruled out in the present inspection.

Overall, the agreement rate between GPR inspection and borehole verification reached 90%, validating the effectiveness and reliability of this technology for emergency inspection of subsurface road defects. At the same time, the limitations were also revealed: strong reflection signals from heterogeneous media such as gravel fill layers can interfere with the extraction and interpretation of effective signals, potentially causing missed detection of deep-seated defects. For similar working conditions, it is recommended to integrate multi-source geophysical methods to improve the comprehensiveness and accuracy of inspection results.

5 Technical Advantages and Limitations of GPR

5.1 Advantages

High resolution. GPR employs high-frequency pulsed electromagnetic waves for detection. The narrow width of individual electromagnetic pulses enables both high vertical and high lateral resolution simultaneously. When a vehicle-mounted GPR system performs detection at speeds of 40 km/h or higher, the distance sampling interval can be controlled to 1 cm. In the emergency road defect inspection case on a radial road in Guangzhou, the 400 MHz antenna successfully identified a minute void anomaly with a depth of only 0.08 m (Anomalous Zone No.1), fully demonstrating the high-resolution capability of this technology.

High efficiency. The sampling and signal reception duration of GPR is extremely short, and the antenna does not require direct contact with the detection surface, enabling rapid inspection operations. In the aforementioned radial road inspection case, a single coverage inspection of a 4-lane × 60 m area required only approximately 30 minutes, with minimal impact on arterial road traffic in the city. This can significantly reduce labor and time costs.

Non-destructive detection. GPR accomplishes the emission and reception of electromagnetic waves entirely through the antenna system. The electromagnetic waves couple into the subsurface medium through the air and complete propagation, and the entire inspection process causes no damage to the existing pavement structure. This makes GPR particularly suitable for periodic health monitoring and emergency defect investigation of in-service roads.

5.2 Limitations

Similar to other geophysical exploration methods, GPR technology has certain limitations:

Inherent trade-off between detection depth and resolution. High-frequency electromagnetic waves offer higher resolution but undergo faster signal attenuation, resulting in shallower effective detection depth. Low-frequency electromagnetic waves have stronger penetration capability, enabling deeper detection, but at the cost of reduced resolution. In practical engineering inspections, multi-frequency antenna combinations are commonly adopted to mitigate this contradiction.

Performance degradation under high-moisture conditions. The relative permittivity of water ($\varepsilon_r \approx 81$) is much higher than that of common construction materials in road engineering. When the moisture content of the medium in the detection area increases, electromagnetic wave attenuation intensifies significantly. The radial road engineering case demonstrated that grouting operations and rainfall events increased the subsurface soil moisture content, causing a marked increase in radar signal noise below 0.6–0.9 m depth, with detection performance deteriorating sharply. Furthermore, strong reflection signals produced by heterogeneous media such as gravel fill layers also interfere with the extraction and interpretation of effective signals. For such working conditions, it is recommended to conduct GPR re-inspection 72 hours after the completion of borehole grouting, or to integrate complementary geophysical methods such as high-density electrical resistivity tomography to improve the reliability of inspection results.

6 Conclusions

This study focuses on Ground Penetrating Radar (GPR) technology and systematically examines its application methods in pavement layer thickness measurement, subsurface defect identification, underground pipeline detection, and tunnel lining quality inspection. Using the emergency inspection of an embankment collapse on a radial road in Guangzhou as an engineering case study, the full-process practice of GPR detection–borehole verification reveals the detection effectiveness and applicability boundaries of GPR in road collapse emergency scenarios. The main conclusions are as follows:

Pavement layer thickness measurement: GPR can effectively achieve large-area rapid inspection of pavement structural layer thickness, with vertical resolution reaching ±3 mm. By fitting permittivity values with a normal distribution and constructing a thickness acceptance probability model, the measurement error can be reduced to ±1.5 mm, and the section acceptance qualification rate can be improved to 98%, significantly outperforming the conventional point-to-area extrapolation method of core drilling.

Subsurface defect identification: Different types of defects exhibit distinct waveform and reflection-event response characteristics in GPR images. Water-rich zones show strong top-interface reflections with significant signal attenuation below; loosened soil zones display interrupted lateral continuity of reflection events and disordered waveforms; void zones present two clearly distinguishable upper and lower reflection interfaces with irregular strong reflections between layers; cavity zones combine weak-reflector characteristics with combined top-and-bottom interface reflection responses. These characteristics provide a reliable basis for rapid defect classification.

Emergency inspection effectiveness: In the emergency inspection case of the embankment collapse on a radial road in Guangzhou, GPR identified 5 anomalous zones

in the first inspection. Through 16 rounds of dynamic inspection over 7 days, a cumulative total of 17 anomalous zones was identified, with the largest composite anomalous area reaching 472 m². Borehole verification results showed that 9 out of 10 boreholes near the collapse zone revealed loosened strata or voids, corresponding to a GPR detection accuracy of 90%, validating the effectiveness of the "GPR detection–borehole verification–grouting treatment–monitoring verification" emergency inspection workflow.

Technical limitations: GPR exhibits an inherent trade-off between detection depth and resolution. Under high-moisture conditions, electromagnetic wave signal attenuation is severe, and detection performance below 0.6–0.9 m depth deteriorates significantly. Strong reflection signals from heterogeneous gravel fill layers interfere with effective signal extraction and may cause missed detection of deep-seated defects. It is recommended to conduct GPR re-inspection 72 hours after grouting completion or to integrate complementary geophysical methods such as high-density electrical resistivity tomography to improve detection reliability under complex working conditions.

Overall assessment: By virtue of its significant advantages of high resolution, high efficiency, and non-destructive detection, GPR has become an indispensable technical tool in highway construction quality control and operational maintenance inspection. In the future, through the optimization of intelligent algorithms, multi-source data fusion, and standardization system development, the detection reliability of GPR under complex working conditions is expected to be further improved, driving the transition of road inspection from qualitative assessment to quantitative evaluation and providing scientific support for full-life-cycle road management.

Acknowledgments

This research is funded by the Guangdong Jianke Traffic Engineering Quality Inspection Center Co., Ltd. for the development and research of the Jianke Traffic Intelligent Agent Platform based on Large Language Model (LLM) (0101RDN2025JT0000820).

Disclosure of Interests. The authors have no competing interests to declare that are relevant to the content of this article.

References

1. Lee, T., Lee, H.M., Hong, J., et al.: Influence of antenna polarization and moisture content on detection of GFPR bars in concrete using ground penetrating radar. NDT and E International 158, 103574 (2026).
2. Almalki, M.A., Almutairi, K.F: Inspection of reinforced concrete structures using ground penetrating radar: Experimental approach. Journal of King Saud University - Science 36(4), 103140 (2024).
3. Chang, C.-W., Tsai, C.-A., Shiau, Y.-C.: Inspection of Steel Bars Corrosion in Reinforced Concrete Structures by Nondestructive Ground Penetrating Radar. Applied Sciences 12(11), 5567 (2022).
4. Yang, H., Guo, K., Zhang, J., et al.: High-precision quantitative detection of subgrade defects in GPR images via deep learning. Measurement 277, 121555 (2026).

5. Fang, L., Yang, F., Fang, Y., et al.: Multi-Frequency GPR Image Fusion Based on Convolutional Sparse Representation to Enhance Road Detection. Journal of Imaging 12(1), 52 (2026).
6. Zhang, B., Xu, S., Zhong, Y., et al.: Three-dimensional reconstruction of loose defects in semi-rigid base layers using enhanced deep learning and point cloud from GPR images. Computer-Aided Civil and Infrastructure Engineering 40(31), 6475-6492 (2025).
7. Wenliang, Z., Gongfeng, X., Guanxu, L., et al.: Ground penetrating radar forward modeling of roads based on random media model. Acta Geodaetica et Geophysica 58(1), 109-122 (2023).
8. Abdelmawla, A., Yang, J.J., Kim, S.S.: Field Validation of Deep-Learning-Based Ground Penetrating Radar Image Analysis for Advancing Subsurface Distress Detection. Transportation Research Record 2678(11), 489-500 (2024).

Open Access This chapter is licensed under the terms of the Creative Commons Attribution-NonCommercial 4.0 International License (http://creativecommons.org/licenses/by-nc/4.0/), which permits any noncommercial use, sharing, adaptation, distribution and reproduction in any medium or format, as long as you give appropriate credit to the original author(s) and the source, provide a link to the Creative Commons license and indicate if changes were made.

The images or other third party material in this chapter are included in the chapter's Creative Commons license, unless indicated otherwise in a credit line to the material. If material is not included in the chapter's Creative Commons license and your intended use is not permitted by statutory regulation or exceeds the permitted use, you will need to obtain permission directly from the copyright holder.

